BIOCHEMISTRY
including biophysical chemistry & molecular biology
Article

Biochemistry **2010,** *49,* 4255–4263 4255
DOI: 10.1021/bi100323v

Thermodynamic Consequences of Incorporating 4-Substituted Proline Derivatives into a Small Helical Protein[†]

Tong-Yuan Zheng,[‡] Yu-Ju Lin,[‡] and Jia-Cherng Horng*

Department of Chemistry, National Tsing Hua University, Hsinchu, Taiwan 30013, ROC
[‡]*These authors contributed equally to this work*

Received March 4, 2010; Revised Manuscript Received April 17, 2010

ABSTRACT: Although proline residues are incompatible with an α-helix conformation, they fit well into the N-terminal end of α-helices. Proline can form either a C^{γ}-*exo* ring pucker or a C^{γ}-*endo* ring pucker. An electron-withdrawing substituent on the 4*R* position of proline favors an *exo* ring pucker while an *endo* ring pucker is preferred if the substituent is on the 4*S* position due to stereoelectronic effects. The villin headpiece subdomain (HP36) is a small helical protein composed of three α-helices and contains a proline residue (Pro62) at the N-terminus of its C-terminal α-helix. Pro62 has a C^{γ}-*exo* ring pucker and forms an aromatic−proline interaction, with Trp64 in the native structure. This work reports the use of 4-substituted proline derivatives, including (2*S*,4*R*)-4-hydroxyproline (Hyp), (2*S*,4*R*)-4-fluoroproline (Flp), (2*S*,4*R*)-4-methoxyproline (Mop), (2*S*,4*S*)-4-hydroxyproline (hyp), (2*S*,4*S*)-4-fluoroproline (flp), and (2*S*,4*S*)-4-methoxyproline (mop), to replace Pro62 and study how the pucker conformation affects the proline−aromatic interaction and the stability of HP36. CD and NMR measurements indicate that all of the HP36 variants incorporated with proline derivatives maintain a structure similar to that of the wild type. Thermal unfolding and urea-induced denaturation measurements have shown that all of the mutants with the exception of the one with the flp substitution are less stable than the wild type. Our results reveal that, upon the replacement of Pro62 to proline derivatives, not only do stereoelectronic effects influence the aromatic−proline interaction but the steric and hydrophobic effects induced by the substituents also play an important role in modulating the stability of HP36.

Noncovalent forces play a critical role in protein structures. These forces include hydrogen bonds, electrostatic interactions, cation−π interactions, aromatic−proline interactions, and hydrophobic interactions. Among these interactions, aromatic−proline interactions are regarded as being one of the nonconventional forces involving proline ring C−H groups and aromatic π-electrons (C−H$\cdots\pi$) (*1*). According to the analysis of protein chains in PDB files, approximately 45% of proline residues in proteins are involved in aromatic−proline interactions (*1*). Specifically, such interactions have been observed to contribute to the structural stability of a few miniproteins (*2*−*6*). One is the villin headpiece subdomain (HP36),[1] and as shown in Figure 1, an aromatic−proline interaction exists between Pro62 and Trp64. HP36 is the helical C-terminal domain from the villin headpiece and can fold cooperatively in isolation (*7*−*9*). It is also one of the smallest known naturally occurring proteins which folds into a compact native structure (*10*) and has been shown to fold on the microsecond time scale (*11*, *12*). As shown in Figure 1, HP36 consists of three short α-helices which pack to form a hydrophobic core composed of three Phe residues and other residues (*8*, *9*). The importance of the hydrophobic core has been investigated in previous studies (*13*, *14*), and a replacement of Phe residues to fluoro-aromatic acids has also been performed to stabilize the structure (*15*, *16*). Although it has been demonstrated that the aromatic−proline interaction between Trp64 and Pro62 considerably contributes to the stability of HP36 (*6*, *14*), this has not been examined in detail. As shown in Figure 1, the distance between the pyrrolidine ring of Pro62 and the indole ring of Trp64 is within 3 Å, which should generate a strong aromatic−proline interaction (*1*). Installing substituents on the pyrrolidine ring of the proline would provide a possibility of modulating this interaction and the structural stability.

Proline often plays a critical role in protein structures due to the conformational constraints imposed by its five-membered pyrrolidine ring (*17*). The ring constraint often restricts the backbone torsion ϕ angles to around −60°, making Pro ideal for a location in β-turns (*18*, *19*) and at the N-terminal end of α-helices (*20*). Proline can form either a C^{γ}-*exo* ring pucker, in which C^{γ} is puckered toward the C^{α} proton, or a C^{γ}-*endo* ring pucker, in which C^{γ} is puckered toward the carbonyl group. The installation of an electron-withdrawing substituent on C4 of the pyrrolidine ring alters the relative energies of the conformers, and this can lead to the bias of a single conformer due to a gauche effect (*21*, *22*). As shown in Figure 1, an *exo* pucker is favored when an electron-withdrawing group (OH, F, or OMe) is in the 4*R*

[†]Supported by the Taiwan National Science Council (Grants NSC 97-2113-M-007-008-MY2 and NSC 98-2119-M-007-011).

*To whom correspondence should be addressed: phone, 886-3-5715131 ext 35635; fax, 886-3-5711082; e-mail, jchorng@mx.nthu.edu.tw.

[1]Abbreviations: CD, circular dichroism; HP36, the villin headpiece subdomain; Hyp, three-letter code for (2*S*,4*R*)-4-hydroxyproline; Flp, three-letter code for (2*S*,4*R*)-4-fluoroproline; Mop, three-letter code for (2*S*,4*R*)-4-methoxyproline; hyp, three-letter code for (2*S*,4*S*)-4-hydroxyproline; flp, three-letter code for (2*S*,4*S*)-4-fluoroproline; mop, three-letter code for (2*S*,4*S*)-4-methoxyproline; Fmoc, *N*-9-fluorenylmethoxycarbonyl; HBTU, *O*-benzotriazole-*N*,*N*,*N*′,*N*′-tetramethyluronium hexafluorophosphate; TOCSY, total correlation spectroscopy; NOESY, nuclear Overhauser effect spectroscopy.

© 2010 American Chemical Society
Published on Web 04/20/2010

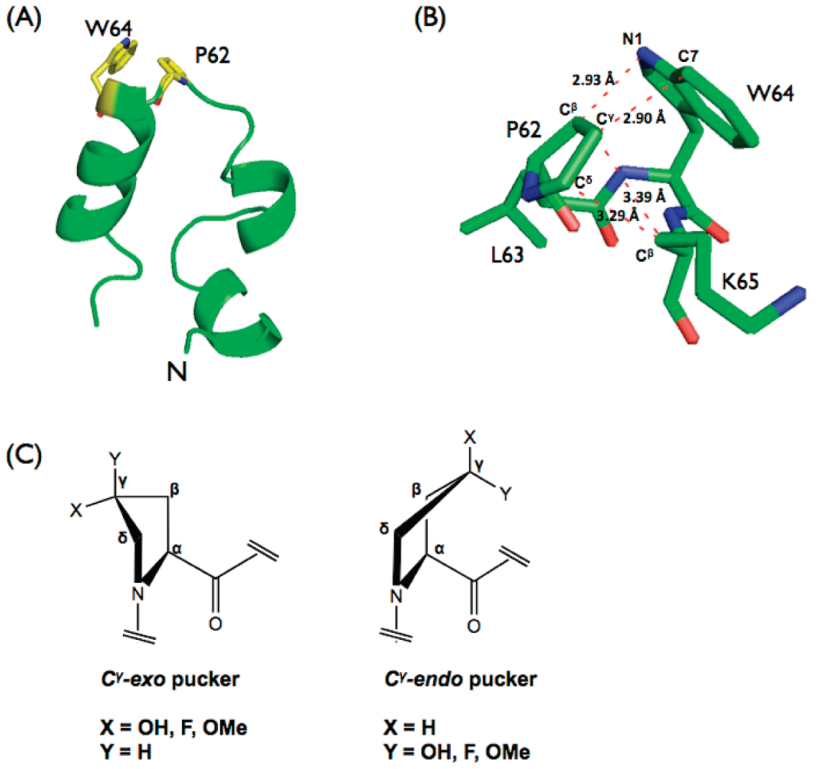

FIGURE 1: (A) Structure of the chicken villin headpiece subdomain, HP36. The ribbon diagram was created using the PyMol program (http://pymol.sourceforge.net) and PDB file 1VII. The N-terminus, Pro62, and Trp64 are labeled. (B) Stick diagram of the PLWK sequence. The distance between the pyrrolidine ring of Pro62 and the indole ring of Trp64 and the distance between C^{γ} of Pro62 and C^{β} of Lys65 are indicated. (C) Ring conformation of Pro and 4-substitued Pro derivatives. The ring conformational preferences depend on the stereochemistry and electronic effects of the substitution: C^{γ}-*exo* pucker is favored when an electron-withdrawing group is on X (Hyp, Flp, Mop) while C^{γ}-*endo* pucker is favored when an electron-withdrawing group is on Y (hyp, flp, mop).

position while an *endo* pucker is preferred when the substituent is in the 4*S* position. The proline ring pucker constrains the ϕ, ψ, and ω main chain torsion angles, and thus, a selective control of the ring pucker provides the possibility of preorganizing the protein backbone conformation and modulating the protein stability (*21*). In fact, it has been previously reported that the installation of proline derivatives with a biased ring pucker can selectively stabilize or destabilize the proteins or peptides, including collagen (*21*−*24*), polyproline helices (*25*−*27*), elastin mimics (*28*), and the Trp-cage miniprotein (*29*).

Of the above studied proteins and peptides, Trp-cage is a 20-residue helical protein in which the proline substituted (Pro12) is located at the C-terminal end of the α-helix and is not involved in other interactions (*29*). In contrast, HP36 has only one proline residue which is located at the N-terminal end of its C-terminal α-helix and is involved in an aromatic−proline interaction. In the native structure, the dihedral angles (ϕ, ψ) of Pro62 are −58.26° and 146.67°, which is typical of an *exo* pucker conformation (*21*) although the displacement of the C^{γ} atom from the ring plane is not very large. Pro62 is also the last residue of the turn connecting the second and third α-helices. These unique features of Pro62 in HP36 imply that it may play a special role in forming a strong aromatic−proline interaction and in contributing to the structural stability. In addition, no studies have been reported to examine how the stereoelectronic effects of a proline residue affect its adjacent C-terminal α-helix. This is what attracts us to explore the relationship between stereoelectronic effects, the ring pucker conformation of Pro62, the aromatic−proline interaction, and the stability of HP36 and to examine whether the ring puckering persists as a decisive stabilizing element when the proline residue participates in additional interactions. To investigate the folding consequences of incorporating 4-substituted proline derivatives into HP36, we herein have prepared a series of HP36 variants in which Pro62 is replaced by (2*S*,4*R*)-4-hydroxyproline (Hyp), (2*S*,4*R*)-4-fluoroproline (Flp), (2*S*,4*R*)-4-methoxyproline (Mop), (2*S*,4*S*)-4-hydroxyproline (hyp), (2*S*,4*S*)-4-fluoroproline (flp), or (2*S*,4*S*)-4-methoxyproline (mop). From CD and NMR spectra, we find that the incorporation of 4-substituted proline derivatives does not significantly disturb the structure. Thermal unfolding and urea denaturation measurements indicate that all 4-substituted proline derivatives with the exception of flp destabilize HP36. Our results suggest that either an *exo* or *endo* ring pucker weakens the aromatic−proline interaction between Trp64 and Pro62. Furthermore, upon the introduction of proline derivatives the hydrophobic and steric effects induced by the substituted group on C4 would also contribute to stabilizing or destabilizing the structure. Our findings provide a valuable insight into how stereoelectronic effects interplay with aromatic−proline interactions and modulate the protein stability, which could be useful when designing proteins and tuning protein stability.

MATERIALS AND METHODS

General. Reagents were obtained from Aldrich Chemical, Alfa Aesar, Fluka, Novabiochem, or Sigma and used without further purification. Amino acids were obtained from Advanced ChemTech, and Fmoc-(2*S*,4*R*)-4-fluoroproline was obtained from Bachem Bioscience. Fmoc-(2*S*,4*S*)-4-fluoroproline, Fmoc-(2*S*,4*S*)-TBDMS-4-hydroxyproline, Fmoc-(2*S*,4*R*)-4-methoxyproline, and Fmoc-(2*S*,4*S*)-4-methoxyproline were synthesized as described previously (*25*). ESI-MS spectra were obtained using

a Q-TOF LC/MS/MS (Micromass Inc.) spectrometer at the National Chiao Tung University Precious Instrument Center. NMR spectra for monitoring the synthesis of proline derivatives were recorded with a Varian INOVA-500 spectrometer.

Peptide Synthesis and Purification. All peptides were prepared on a 0.1 mmol scale by a standard solid-phase method using Fmoc-protected amino acids, HBTU-mediated coupling, and standard reaction cycles on an automated PS3 peptide synthesizer (Protein Technologies Inc.). All β-branched amino acids and all residues coupling to β-branched amino acids were double coupled. Use of a Rink amide resin with a MBHA linker generated an amidated C-terminus following cleavage from the resin with 92.5% trifluoroacetic acid (TFA)/2.5% triisopropylsilane/2.5% H_2O/2.5% ethanedithiol. All peptides were purified by reverse-phase HPLC with a Thermo Biobasic semipreparative C18 column. H_2O/acetonitrile gradients with 0.1% (v/v) TFA as the counterion were used for the purification. All peptides were >90% pure according to HPLC analysis. The identities of all peptides were confirmed by using ESI-MS. The calculated and observed molecular masses were as follows: WT-HP36, calculated 4188.17, observed 4188.73; Hyp-HP36 calculated 4202.18, observed 4202.15; Flp-HP36 calculated 4204.18, observed 4203.99; Mop-HP36 calculated 4216.74, observed 4215.31; hyp-HP36 calculated 4202.18, observed 4202.72; flp-HP36 calculated 4204.18, observed 4203.99; mop-HP36 calculated 4216.74, observed 4215.20.

Circular Dichroism (CD) Spectroscopy. CD experiments were performed with an Aviv Model 410 CD spectrometer. Far-UV CD spectra were obtained at 25 °C in 10 mM sodium acetate and pH 5.0 buffer using a 1 mm path length quartz cuvette. Thermal denaturation and urea-induced unfolding experiments were performed in a 1 cm path length quartz cuvette by monitoring the signal at 222 nm. Thermal unfolding experiments were performed from 2 to 98 °C with a 2 °C interval. The reversibility of thermal denaturations for HP36 and its variants was more than 95%. Reversibility was judged by the recovery of the signal at 25 °C after heating the protein solution at 98 °C for 5 min. Urea-induced denaturation was conducted at 25 °C, and the urea concentration in solution was determined by measuring the refractive index. The protein concentrations were 100 μM for far-UV CD measurements and 10−50 μM for unfolding experiments. Protein concentrations were determined by absorbance measurement in 6 M guanidine hydrochloride at pH 6.5 using the extinction coefficient (ε) 5690 M^{-1} cm^{-1} at 280 nm.

Fluorescence Spectroscopy. Fluorescence spectra were recorded on a HITACHI F-4500 fluorescence spectrophotometer. All measurements were conducted at room temperature (~25 °C) in 10 mM sodium acetate and pH 5.0 buffer using a 1 cm quartz cuvette. The bandwidth was 2.5 nm for excitation and 5.0 nm for emission. The protein concentration was 10 μM. The excitation wavelength was 280 nm, and the emission spectra were recorded from 290 to 600 nm.

Urea and Thermal Denaturation Curve Fitting. Urea denaturation curves were fit using standard methods (*30*). A two-state model was used to fit data collected from CD experiments to determine protein stability, $\Delta G°_U(H_2O)$, in the absence of urea. The data were fit to the equation:

$$\theta = (\theta_N + \theta_U \exp(-\Delta G°_U/RT))/(1 + \exp(-\Delta G°_U/RT)) \quad (1)$$

where θ is the measured ellipticity from CD, θ_N is the ellipticity of the native state, θ_U is the ellipticity of the denatured state, and θ_N and θ_U are given by

$$\theta_N = a + b[\text{urea}] \quad (2a)$$

$$\theta_U = c + d[\text{urea}] \quad (2b)$$

where the four parameters, a, b, c, d, are used to define the ellipticity of the native and denatured state. The free energy of unfolding is assumed to be a linear function of denaturant concentration:

$$\Delta G°_U = \Delta G°_U(H_2O) - m[\text{urea}] \quad (3)$$

where $\Delta G°_U$ is the apparent free energy for the native to denatured transition. Thermal unfolding data were also fit by assuming that the folded and unfolded baselines are a linear function of absolute temperature (T). An expression similar to eq 1 was used but with the denaturant concentration substituted by absolute temperature. The temperature dependence of $\Delta G°_U$ is described by the Gibbs−Helmholtz equation:

$$\Delta G°_U(T) = \Delta H°(T_m)(1 - T/T_m) - \Delta C_p°[(T_m - T) + T \ln(T/T_m)] \quad (4)$$

where $\Delta G°_U(T)$ is the free energy of unfolding, T_m is the unfolding midpoint temperature, $\Delta H°(T_m)$ is the enthalpy change at T_m, and $\Delta C_p°$ is the heat capacity change between the native and denatured states. The $\Delta C_p°$ of wild-type HP36 used in the previous study (*14*), 0.38 kcal mol^{-1} deg^{-1}, was used to determine T_m for all proteins. Note that the exact value of T_m is not sensitive to the choice of $\Delta C_p°$.

Nuclear Magnetic Resonance (NMR) Spectroscopy. NMR experiments were performed on a Varian VNMRS 700 MHz or a Bruker DMX 600 MHz spectrometer at the National Tsing Hua University Instrumentation Center. All spectra were internally referenced to sodium 3-(trimethylsilyl)propionate-*2,2,3,3-d*$_4$ (TSP) at 0.0 ppm. 1D and 2D spectra were taken at 2 mM protein concentration at 25 °C in 90% H_2O/10% D_2O, 10 mM phosphate, and 150 mM NaCl buffer at pH 5.0. TOCSY and NOESY spectra were used for assignments. A mixing time of 75 ms was used in the TOCSY experiments, and 250 ms was used in the NOESY experiments. The deviation of the chemical shifts of the C_α protons from random coil values was calculated using the random coil chemical shifts of Wüthrich (*31*). Native state chemical shifts for HP36 are from McKnight et al. (*7*).

RESULTS

Design of HP36 Variants. In order to investigate how stereoelectronic effects influence the aromatic−proline interaction and the folding stability of the villin headpiece subdomain, HP36, we designed a series of HP36 variants in which the proline residue (Pro62) was replaced by various 4-substituted proline derivatives. Since the stereochemistry and inductive effects of the substitution affect the C^γ ring pucker conformation (*21*−*23*), we chose electron-withdrawing groups, including OH, F, and OMe, as the substituent on C4 of proline. The C^γ ring pucker preference of Pro62 imposed by these groups on different stereochemical positions was expected to affect the local interactions. The electron-withdrawing groups, OH, F, and OMe, on the C^γ of proline can also make the adjacent CH groups more positive and strengthen the C−H$\cdots\pi$ interaction between Pro62 and Trp64. Moreover, the distance between the pyrrolidine ring of Pro62 and the indole ring of Trp64

Table 1: Amino Sequences of HP36 and Its Variants

Protein	Sequence[a]
	41 50 60 70[b]
WT-HP36	NH_3-MLSDEDFKAVFGMTRSAFANL**Pro**LWKQQNLKKEKGLF-NH_2
Hyp-HP36	NH_3-MLSDEDFKAVFGMTRSAFANL**Hyp**LWKQQNLKKEKGLF-NH_2
Flp-HP36	NH_3-MLSDEDFKAVFGMTRSAFANL**Flp**LWKQQNLKKEKGLF-NH_2
Mop-HP36	NH_3-MLSDEDFKAVFGMTRSAFANL**Mop**LWKQQNLKKEKGLF-NH_2
hyp-HP36	NH_3-MLSDEDFKAVFGMTRSAFANL**hyp**LWKQQNLKKEKGLF-NH_2
flp-HP36	NH_3-MLSDEDFKAVFGMTRSAFANL**flp**LWKQQNLKKEKGLF-NH_2
mop-HP36	NH_3-MLSDEDFKAVFGMTRSAFANL**mop**LWKQQNLKKEKGLF-NH_2

[a] NH_3 denotes a free N-terminus, and NH_2 denotes an amidated C-terminus. Hyp is (4*R*,2*S*)-4-hydroxyproline, hyp is (4*S*,2*S*)-4-hydroxyproline, Flp is (4*R*,2*S*)-4-fluoroproline, flp is (4*S*,2*S*)-4-fluoroproline, Mop is (4*R*,2*S*)-4-methoxyproline, and mop is (4*S*,2*S*)-4-methoxyproline. [b] The numbering system corresponds to that used for the full-length villin headpiece.

is within 3 Å, and thus, the insertion of these groups allows us to examine whether any significant steric strains are induced in the structure due to the substituted groups. Three 4*R*-substitued proline derivatives, (2*S*,4*R*)-hydroxyproline (Hyp), (2*S*,4*R*)-fluoroproline (Flp), and (2*S*,4*R*)-methoxyproline (Mop), and their 4*S* stereoisomers, (2*S*,4*S*)-hydroxyproline (hyp), (2*S*,4*S*)-fluoroproline (flp), and (2*S*,4*S*)-methoxyproline (mop), were used to replace the Pro62 of HP36. The wild-type and mutated proteins studied in this report are designated as WT-HP36, Hyp-HP36, Flp-HP36, Mop-HP36, hyp-HP36, flp-HP36, and mop-HP36, and their amino sequences are shown in Table 1. All peptides are chemically synthesized and have a free N-terminus and an amidated C-terminus.

All 4-Substituted Proline Derivatives Incorporated in HP36 Variants Maintain a Structure Similar to That of the Wild Type. The far-UV CD spectra for wild-type HP36 and its variants were measured at 25 °C. As shown in Figure 2, all mutants have a far-UV CD spectrum similar to that of wild-type HP36 and show a highly α-helical structure. We also performed CD measurements at different protein concentrations for HP36 and its variants. Their CD spectra are concentration independent (shown in the Supporting Information Figure S1), indicating that these proteins are monomeric in solution. To further examine whether or not the mutated proteins have a well-folded structure, we measured their ^{1}H NMR spectra. Both one- and two-dimensional NMR spectra were recorded at 25 °C. The one-dimensional ^{1}H NMR spectra show that all HP36 variants exhibit well-dispersed resonances and a pattern similar to that of WT-HP36 (Figure 3). More specifically, as shown in Figure 3, a well-resolved upfield resonance at −0.11 ppm, which corresponds to the methyl group of Val50 in the native HP36 structure (*12*), appears in each spectrum, indicating that all mutants have a structure similar to that of wild-type HP36. We further used the TOCSY and NOESY spectra to assign the backbone proton chemical shifts of all mutants. Except for Flp-HP36, the backbone assignments for 32 of the 36 residues could be made for the HP36 mutants. As shown in Figures 4 and 5, the observed C^α proton chemical shifts are similar to those of the wild type. Deviations from the chemical shifts measured in wild-type HP36 are mainly within ±0.15 ppm, while the deviations from random coil values are much larger, ranging up to +0.4 and −1.1 ppm. For the Flp-HP36 variant, although less backbone C^α proton chemical shifts could be assigned due to its less resolved NMR

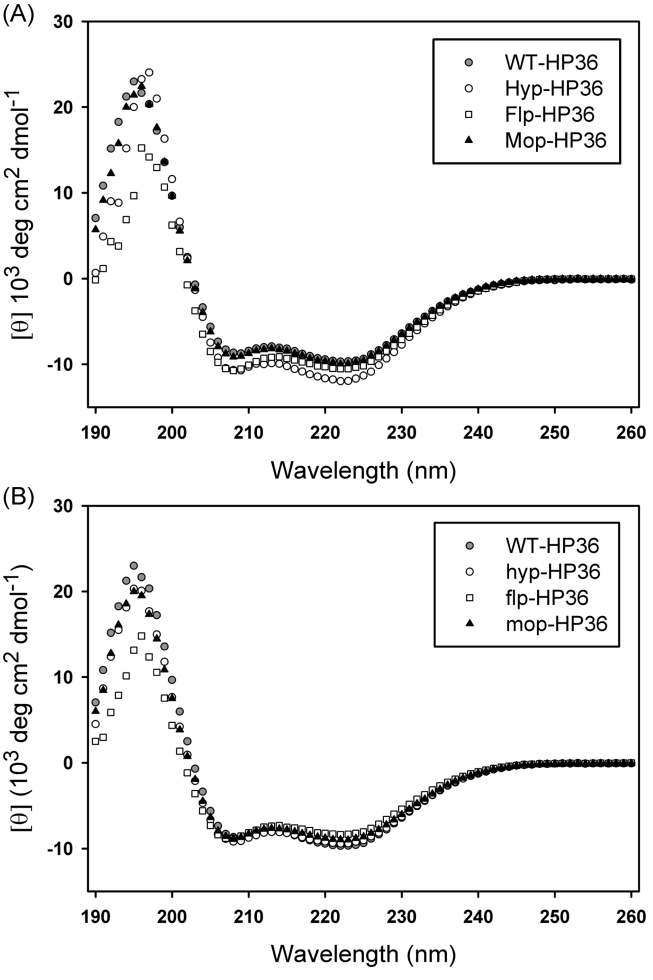

FIGURE 2: Far-UV CD spectra for HP36 and its variants at 25 °C. (A) Variants incorporated with 4*R*-substituted proline derivatives. (B) Variants incorporated with 4*S*-substituted proline derivatives. All measurements were conducted in 10 mM sodium acetate at pH 5.0.

spectra, the chemical shift deviations from the wild type and the random coil are in a similar pattern to the other five mutants. The large negative deviations from the random coil values in three regions (residues 44−51, 55−59, and 63−72) demonstrate that the variants form α-helical structure on these sites, consistent with the native structure of wild-type HP36. The existence of three

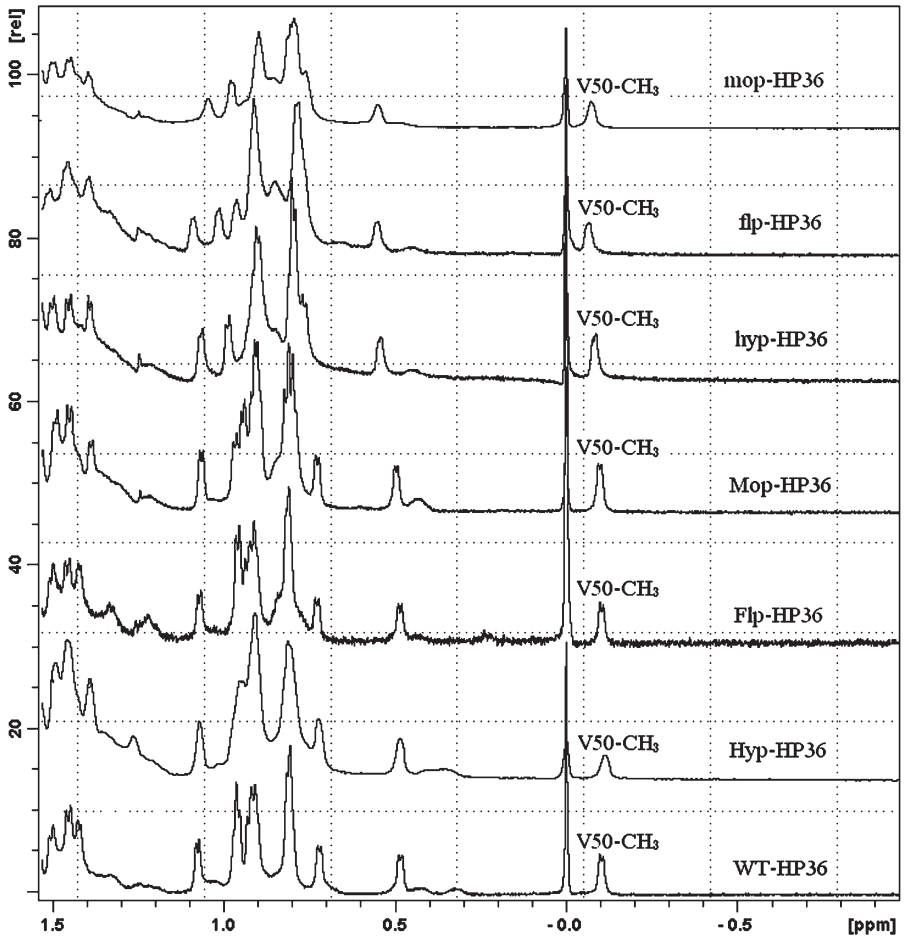

FIGURE 3: Stacked plots of the upfield region of the 1D ^{1}H NMR spectra of wild-type HP36 and its mutants. The upfield chemical shifts of V50 methyl groups (below 0 ppm) confirm that all of the mutants are folded. All spectra were recorded at 25 °C and pH 5.0 in 90% H_2O/10% D_2O, 10 mM sodium acetate, and 150 mM NaCl.

α-helices confirms that the mutants maintain a secondary structure similar to that of wild-type HP36.

We could not assign the resonances for all aromatic protons of Trp64 due to the lack of very high solution spectra, but the NOE cross-peaks between $C^{\gamma}H$ of Pro derivatives and one aromatic H of Trp64 for the mutants were observed. These NOE cross-peaks indicate the close proximity between the side chains of Pro derivatives and Trp64. The corresponding region of the NOESY spectrum for each HP36 mutant is shown in the Supporting Information (Figure S2). Moreover, it can be noted from the deviations between mop-HP36 and WT-HP36 that the $C^{\alpha}H$ resonance of Lys65 is largely shifted from the wild type, and the deviation is about 0.25 ppm. As shown in Figure 1, the distance between the C^{γ} and C^{δ} atoms of Pro62 and the C^{β} atom of Lys65 is only about 3.4 Å, and an *endo* ring pucker of Pro62 may push C^{γ} atom toward Lys65. All hyp, flp, and mop favor an *endo* ring pucker, which could induce steric strains upon their introduction into HP36. Besides, compared to F and OH groups, the OMe group is much larger, and the large shift of Lys65 in mop-HP36 may be due to the fact that the OMe group at the 4*S* position causes a significant steric clash with the side chain of Lys65 and distorts the main chain torsion angles of Lys65. The close proximity between Pro62 and Lys65 could also be confirmed by the observation of the NOE cross-peaks between $C^{\delta}H$ of Pro derivatives and $C^{\beta}H$ of Lys65 for four of the six mutants. These corresponding NOESY spectra are also shown in Supporting Information (Figure S3). The NMR measurements demonstrate that all six 4-substituted proline derivatives incorporated in HP36 variants maintain a native-like structure.

Besides CD and NMR spectroscopy, Trp fluorescence measurements were performed to examine if the side chain of Trp64 becomes more exposed to solvent upon the replacement of Pro62 to Pro derivatives. A red shift of the emission maximum will indicate that the aromatic residues have become more exposed to solvent. As shown in Table 2, HP36 and its variants have a similar emission maximum ranging from 350 to 356 nm. The emission maxima of the mutants are only slightly red shifted from that of the wild-type protein, indicating that the solvent exposure of Trp64 does not significantly increase in the mutants.

Folding Stability of 4-Substituted Proline Derivatives Incorporated in HP36 Variants. In order to investigate how the incorporation of 4-substituted proline derivatives affects the folding stability of HP36, we conducted thermal unfolding and urea-induced denaturation experiments on the wild-type protein and its mutants. These measurements were carried out by monitoring the CD signals at 222 nm, an index of the changes in α-helical content. As shown in Figures 6 and 7, all of the HP36 mutants fold cooperatively and have an *m*-value similar to that of the wild type. The measured T_m value of WT-HP36 is 61.1 °C at pH 5.0 and the free energy of unfolding ($\Delta G°$) is 2.37 kcal mol^{-1} at 25 °C, which are somewhat slightly lower than previously observed in the chemically synthesized HP36 construct (*12*). All mutants with the exception of flp-HP36 are less stable than

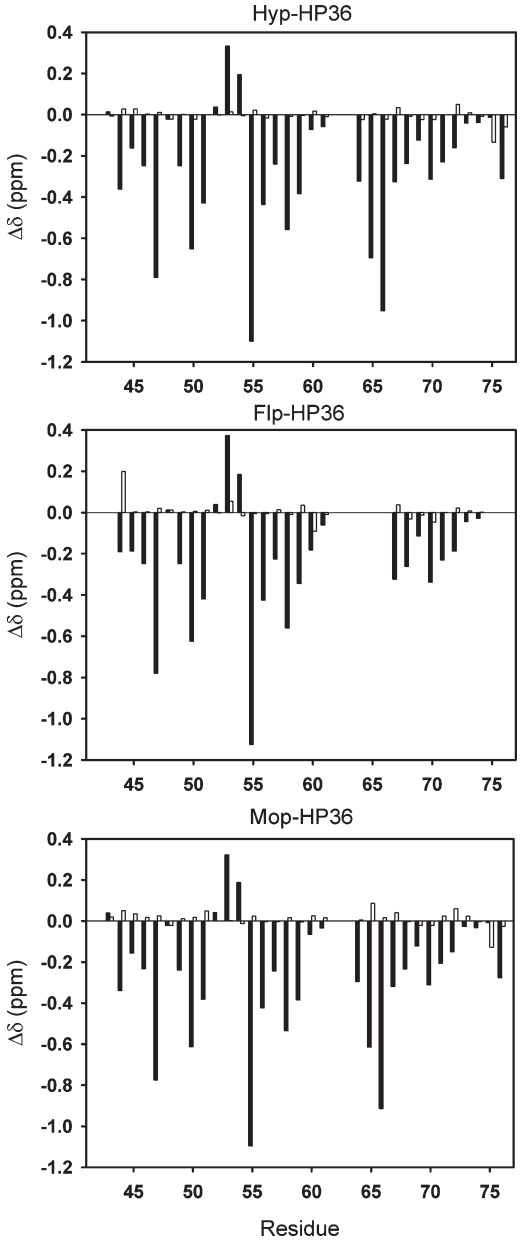

FIGURE 4: Chemical shift deviations between $C^{\alpha}H$ of the HP36 variants incorporated with 4*R*-substituted proline derivatives and wild-type HP36 (empty bars) and chemical shift deviations between $C^{\alpha}H$ of the HP36 variants incorporated with 4*R*-substituted proline derivatives and random coils (full bars).

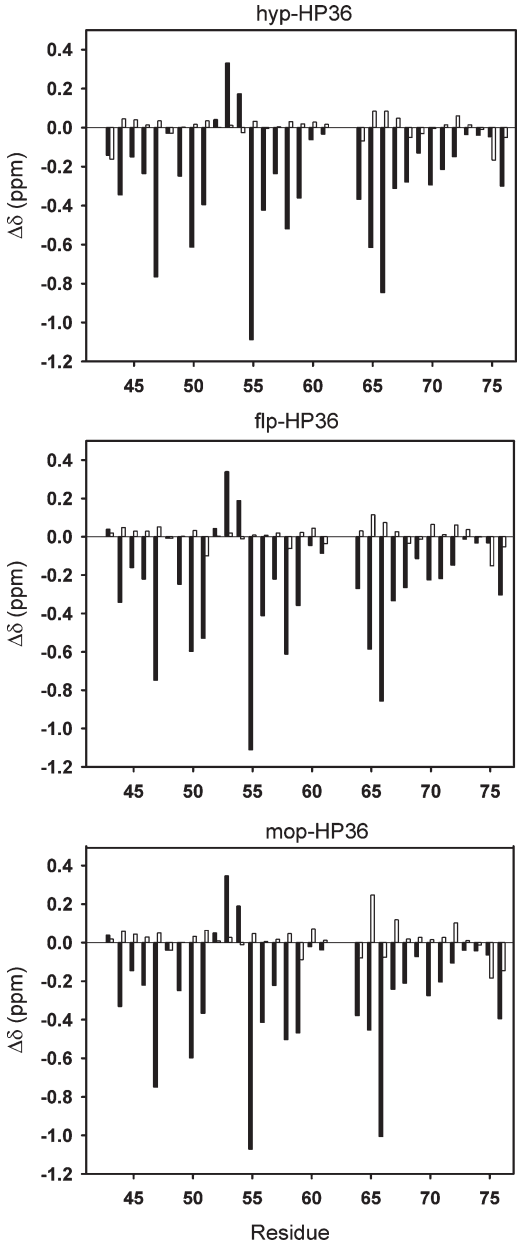

FIGURE 5: Chemical shift deviations between $C^{\alpha}H$ of the HP36 variants incorporated with 4*S*-substituted proline derivatives and wild-type HP36 (empty bars) and chemical shift deviations between $C^{\alpha}H$ of the HP36 variants incorporated with 4*S*-substituted proline derivatives and random coils (full bars).

wild-type HP36, and their folding stability and parameters are summarized in Table 3. Hyp, Flp, and Mop favor a C^{γ}-*exo* ring pucker due to the electron-withdrawing group on the 4*R* position of Pro and were expected to have a positive impact on HP36 since Pro62 adopts a C^{γ}-*exo* ring pucker in the native structure. However, the incorporation of such residues does not stabilize the structure, indicating that the biased *exo* ring pucker does not make the folding of HP36 more favorable. On the other hand, the aromatic−proline interaction between Trp64 and Pro62 may be weakened, since an *exo* ring pucker could make the pyrrolidine ring of Pro62 move away from the indole ring of Trp64, leading to lower stability. Among these three 4*R*-substituted proline derivatives, Flp has the largest destabilizing effect, while Hyp has the least effect on HP36, and they destabilize the structure by 0.97 and 0.29 kcal mol^{-1}, respectively. Flp-HP36 has a free energy of unfolding of about 1.4 kcal/mol, meaning that up to ca. 9% of the peptide could be unfolded at 25 °C. The population of unfolded peptides may result in a less dispersed NMR spectrum, and thus the low stability of Flp-HP36 is consistent with its less resolved $C^{\alpha}H$ resonances.

Table 2: Fluorescence Emission Maximum of HP36 and Its Variants[a]

protein	emission maximum λ (nm)	protein	emission maximum λ (nm)
WT-HP36	350	hyp-HP36	352
Hyp-HP36	352	flp-HP36	355
Flp-HP36	356	mop-HP36	353
Mop-HP36	354		

[a]The measurements were conducted at pH 5.0 in 20 mM sodium acetate buffer at room temperature.

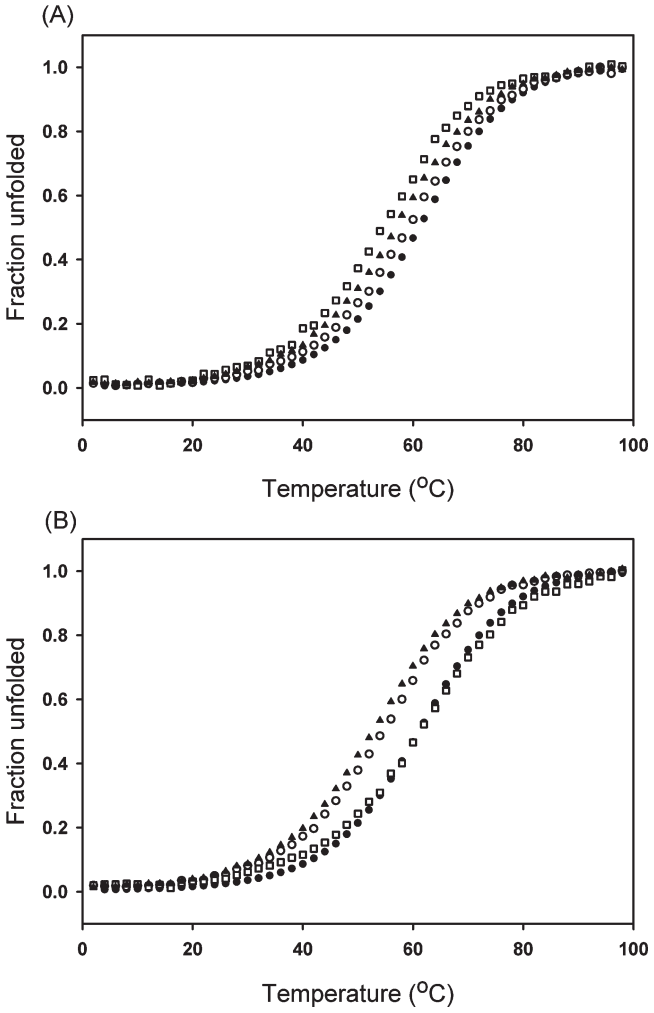

FIGURE 6: Thermal unfolding curves followed by CD measurements at 222 nm for wild-type HP36 (closed circles) and its mutants: (A) Hyp-HP36 (open circles), Flp-HP36 (open squares), and Mop-HP36 (closed triangles); (B) hyp-HP36 (open circles), flp-HP36 (open squares), and mop-HP36 (closed triangles). All measurements were conducted in 10 mM sodium acetate at pH 5.0.

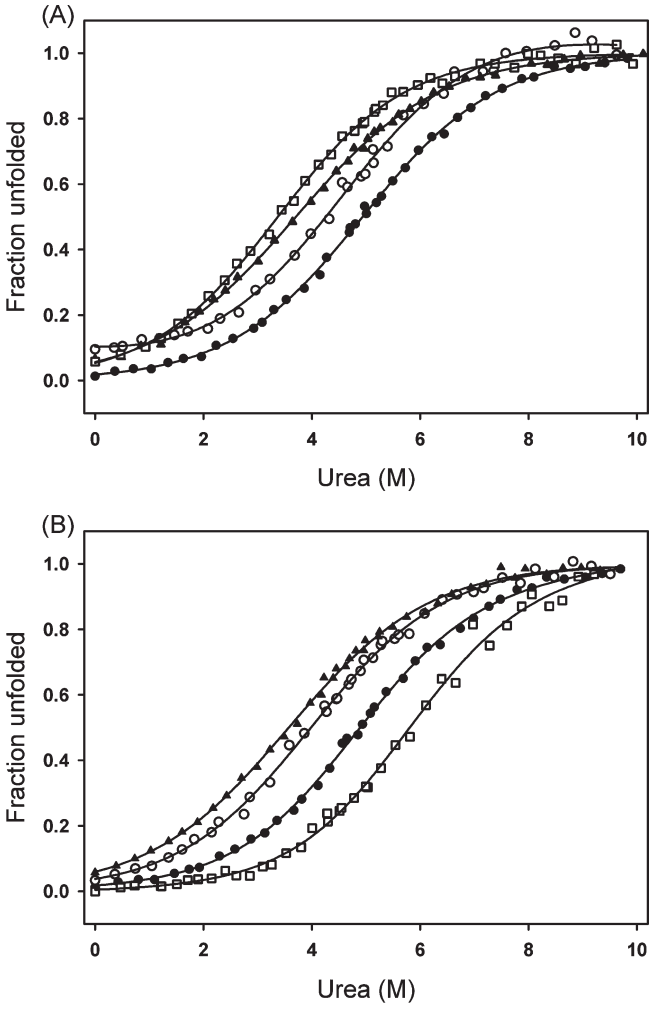

FIGURE 7: Urea-induced denaturation curves followed by CD measurements at 222 nm for wild-type HP36 (closed circles) and its mutants: (A) Hyp-HP36 (open circles), Flp-HP36 (open squares), and Mop-HP36 (closed triangles); (B) hyp-HP36 (open circles), flp-HP36 (open squares), and mop-HP36 (closed triangles). All measurements were conducted at 25 °C and pH 5.0 in 10 mM sodium acetate.

In contrast to 4*R*-substituted proline derivatives, the proline derivatives with an electron-withdrawing group in the 4*S* position of Pro favor a C^{γ}-*endo* ring pucker, and thus, the replacement of Pro62 to hyp, flp, and mop was expected to destabilize HP36 since their preferred *endo* ring pucker is the opposite of the ring pucker conformation adopted by Pro62 in the native structure. As expected, hyp-HP36 and mop-HP36 are less stable than the wild type, and their free energy of unfolding is decreased by 0.64 and 0.73 kcal mol^{-1}, respectively. Strikingly, instead of destabilizing HP36, the incorporation of flp makes the structure slightly more stable. As shown in both Figures 6 and 7 and Table 3, flp-HP36 and WT-HP36 have a similar T_m value, and the unfolding free energy of flp-HP36 is 0.66 kcal mol^{-1} higher than that of WT-HP36. It appears that, although the *endo* ring pucker adopted by flp is not favorable in the native structure, the aromatic−proline interaction is not significantly perturbed by installing F at the 4*S* position of Pro. The results also suggest that the fluoro group does not induce significant steric effects when it moves the ring pucker toward the interior of the structure and that the high hydrophobicity of the C−F group may better fit the environment. Besides, mop-HP36 is less stable than hyp-HP36, indicating that the steric effects imposed by OMe are more significant than those imposed by OH, leading to a larger destabilizing effect. This is also confirmed by the observation of the largely perturbed $C^{\alpha}H$ chemical shift of Lys65 in mop-HP36. It is noted that the trends for T_m values and unfolding free energy (ΔG°_{U}) do not agree perfectly. Tanford and co-workers have presented evidence that proteins could form a more random and disordered structure by chemical denaturations than by thermal denaturations (*32*). A few studies also reported that the protein stability determined by thermal unfolding experiments is not consistent with that by chemical denaturations (*33*, *34*) due to the difference between the thermally unfolded state and the chemically unfolded state. Furthermore, the study of peptide models has provided evidence that there is significant structure in the thermally denatured state of HP36 (*35*). Therefore, the discrepancy between the T_m values and ΔG°_{U} of HP36 and its mutants could be attributed to the different unfolded states upon chemical and thermal denaturations.

DISCUSSION

Different from what was observed to selectively control the stability of Trp-cage using a preorganized ring pucker conformation of proline (*29*), the consequences of introducing proline derivatives into HP36 do not completely correlate with the bias of

Table 3: Thermodynamic Parameters Derived from Thermal Unfolding and Urea-Induced Denaturation for Wild-Type HP36 and Its Variants[a]

protein	T_m (°C)	$\Delta G°_U(H_2O)$ (kcal mol^{-1})	$\Delta\Delta G°_U$[b] (kcal mol^{-1})	*m*-value[b] (kcal mol^{-1} M^{-1})	C_M (M)
WT-HP36	61.1 ± 0.1	2.37 ± 0.20		0.48 ± 0.04	4.94
Hyp-HP36	59.0 ± 0.1	2.08 ± 0.38	−0.29	0.46 ± 0.07	4.52
Flp-HP36	53.8 ± 0.8	1.40 ± 0.36	−0.97	0.42 ± 0.05	3.35
Mop-HP36	56.8 ± 0.1	1.93 ± 0.18	−0.57	0.51 ± 0.03	3.78
hyp-HP36	54.1 ± 0.3	1.93 ± 0.30	−0.64	0.48 ± 0.05	4.02
flp-HP36	60.8 ± 0.6	3.03 ± 0.43	0.66	0.52 ± 0.08	5.83
mop-HP36	52.2 ± 0.4	1.64 ± 0.29	−0.73	0.46 ± 0.05	3.57

[a]The quoted uncertainties in T_m were the standard deviations by averaging repeated measurements. The quoted uncertainties in $\Delta G°_U(H_2O)$ and *m*-value represent the standard errors to the fit. C_M (the [urea] required to reach the midpoint of the transition) was calculated from $\Delta G°_U = \Delta G°_U(H_2O) - m$[urea], when $\Delta G°_U$ is 0. [b]$\Delta\Delta G°_U = \Delta G°_U(H_2O)$ (mutant) − $\Delta G°_U(H_2O)$ (wt).

their pucker conformation. This could be due to the fact that the proline residue substituted in Trp-cage is located at the C-terminus of its α-helix, whereas the proline residue studied here is on the N-terminus of the C-terminal α-helix of HP36. Besides, the proline residue studied in Trp-cage is not involved in the aromatic−proline interactions, while Pro62 does interact with Trp64 via an aromatic−proline interaction. Therefore, it is obvious that the stability of HP36 cannot be selectively controlled by installing an *exo*- or *endo*-biased ring pucker at this position. In the native structure of HP36, the pyrrolidine ring of Pro62 and the indole ring of Trp64 form an edge−face orientation (Figure 1), which generates a strong aromatic−proline interaction (*1*). Although Pro62 adopts an *exo* ring pucker in the native structure, the C^γ atom is only displaced from the ring plane by 0.05 Å to maintain the edge−face orientation between Pro62 and Trp64. This almost nonpuckering of Pro62 strongly suggests that such conformation can make a perfect edge−face arrangement to form a strong aromatic−proline interaction. The importance of this aromatic−proline interaction was also revealed by the fact that singly mutating Trp64 or Pro62 to other amino acids substantially destabilizes the structure (*6*, *14*). Thus a strongly preorganized *exo* ring pucker would push the C^γ atom and the pyrrolidine ring away from Trp64, weakening the aromatic−proline interaction. Of the three 4*R*-substituted Pro derivatives, Flp has the largest destabilizing effect on HP36. The calculation of the solvent-accessible surface area by the program GETAREA (http://curie.utmb.edu/GET.html) shows that the side chain of Pro62 is about 42% exposed to solvent. The substituted group on the 4*R* position of Pro62 should point toward the exterior of HP36, and an *exo* ring pucker would make the side chain even more exposed. Since the organic C−F group is highly hydrophobic, it could induce unfavorable interactions with water in Flp-HP36 when the pyrrolidine ring moves toward the exterior of the protein. This may be why Flp destabilizes HP36 more significantly than Hyp and Mop. Moreover, the electron-withdrawing (*36*) and hyperconjugative abilities (*37*) of OH and OMe are similar, but O-methylation will decrease the hydration of Mop (*38*). Therefore, compared with Hyp, the less hydrated OMe would make Mop less favorable when its ring side chain is exposed to water, leading to a slightly lower stability of Mop-HP36.

For the proline derivatives with an electron-withdrawing group on the 4*S* position, they have a bias to form a C^γ-*endo* ring pucker, and this could cause unfavorable effects upon their incorporation into HP36 since the conformation is opposite to that in the native structure. Both hyp and mop destabilize HP36 as expected. Specifically, hyp and mop destabilize the protein more significantly than their stereoisomers, Hyp and Mop, by 0.15 and 0.29 kcal mol^{-1}. These results strongly suggest that the bias forming an *exo* ring pucker may still contribute to the stability of HP36 to some extent although it could simultaneously perturb the aromatic−proline interaction. The most surprising observation is that flp does not destabilize HP36 as hyp and mop do but slightly stabilizes the protein. It can be rationalized from two aspects: (1) the F group is smaller than the OMe group, causing less steric strain when it moves toward the interior of the protein and the Lys65 residue; (2) the C−F group is more hydrophobic than the C−OH group, making it more favorable in the interior of the protein. Therefore, despite the fact that flp has the bias to form an *endo* pucker which conflicts with the pucker conformation of Pro62 in the native structure and may also weaken the aromatic−proline interaction, its C−F side chain could form strong hydrophobic interactions in the interior of HP36 and compensate for the loss of stability.

Previous studies using conformationally biased proline derivatives to selectively stabilize or destabilize proteins essentially chose the proline residues, which were not involved in other interactions in the structure (*22*, *24*, *28*, *29*). In those cases, a preorganized ring pucker matching the native proline conformation would stabilize the protein; otherwise a destabilizing effect would be observed. In the case of HP36, such stability tuning via a simply conformational bias cannot be independently observed since the proline residue is involved in an aromatic−proline interaction. Any change in the conformation of the proline ring pucker may affect the distance and orientation between aromatic and pyrrolidine rings, which would also affect the strength of the aromatic−proline interaction. An electron-withdrawing group on the pyrrolidine ring should make its adjacent C−H groups more positively charged and enhance the aromatic−proline interaction if the orientation is appropriate. The OH, F, and OMe groups are all electron-withdrawing and could have such effects on the side chain of proline. The 4-substituted proline derivatives used in our current study may provide favorable interactions between the C−H groups of the pyrrolidine ring and the aromatic ring via inductive effects. However, in the native HP36, Pro62 and Trp64 exhibit a nearly perfect edge-to-face orientation, and thus, either an *exo*-favoring or an *endo*-favoring residue will deviate from the edge-to-face orientation and destabilize the aromatic−proline interaction. Our results indicate that disturbing the distance and orientation between Pro62 and Trp64 has a dominant effect in weakening the aromatic−proline interaction, which cannot be compensated by the increase in C−H$\cdots\pi$ interactions due to the inductive effects imposed by F, OH, and OMe.

By incorporating 4-substituted proline derivatives into HP36, we have presented the first example that the biased C^γ ring puckering of proline due to stereoelectronic effects cannot selectively stabilize or destabilize the structure when the proline residue is involved in other interactions. Our data suggest that

the aromatic−proline interaction is significantly perturbed upon the change of the ring pucker conformation. Besides the stereoelectronic effects and the aromatic−proline interaction, the steric strains and hydrophobic effects induced by the substituted groups are involved in the consequences. Specifically, the results from Flp-HP36 and flp-HP36 strongly suggest that the hydrophobicity of the C−F group seems to play a more important role than the stereoelectronic effects of the F group. In conclusion, we have used 4-substituted proline derivatives to reveal that various electron-withdrawing groups on the pyrrolidine ring have different impacts on the small helical protein HP36, and those are the result of a combination of stereoelectronic, steric, and hydrophobic effects and the aromatic−proline interaction. From the study of HP36, we have also demonstrated that the ring puckering cannot remain as a significant stabilizing factor in proteins in which the proline residues take part in additional interactions. Our findings highlight the complicacy of protein structure and the need to consider multiple elements in understanding protein folding stability and, thus, provide a piece of valuable information for designing stable proteins or peptides.

SUPPORTING INFORMATION AVAILABLE

Far-UV CD spectra at different concentrations (Figure S1), excerpts of NOESY spectra (Figures S2 and S3), CD raw data for thermal and chemical denaturations (Figures S4 and S5), and a table listing chemical shifts of NOE cross-peaks (Table S1). This material is available free of charge via the Internet at http://pubs.acs.org.

REFERENCES

1. Bhattacharyya, R., and Chakrabarti, P. (2003) Stereospecific interactions of proline residues in protein structures and complexes. *J. Mol. Biol. 331*, 925–940.
2. Jäger, M., Nguyen, H., Crane, J. C., Kelly, J. W., and Gruebele, M. (2001) The folding mechanism of a β-sheet: the WW domain. *J. Mol. Biol. 311*, 373–393.
3. Macias, M. J., Gervais, V., Civera, C., and Oschkinat, H. (2000) Structural analysis of WW domains and design of a WW prototype. *Nat. Struct. Biol. 7*, 375–379.
4. Neidigh, J. W., Fesinmeyer, R. M., and Andersen, N. H. (2002) Designing a 20-residue protein. *Nat. Struct. Biol. 9*, 425–430.
5. Neidigh, J. W., Fesinmeyer, R. M., Prickett, K. S., and Andersen, N. H. (2001) Exendin-4 and glucagon-like-peptide-1: NMR structural comparisons in the solution and micelle-associated states. *Biochemistry 40*, 13188–13200.
6. Vermeulen, W., Van Troys, M., Bourry, D., Dewitte, D., Rossenu, S., Goethals, M., Borremans, F. A. M., Vandekerckhove, J., Martins, J. C., and Ampe, C. (2006) Identification of the PXW sequence as a structural gatekeeper of the headpiece C-terminal subdomain fold. *J. Mol. Biol. 359*, 1277–1292.
7. McKnight, C. J., Doering, D. S., Matsudaira, P. T., and Kim, P. S. (1996) A thermostable 35-residue subdomain within villin headpiece. *J. Mol. Biol. 260*, 126–134.
8. McKnight, C. J., Matsudaira, P. T., and Kim, P. S. (1997) NMR structure of the 35-residue villin headpiece subdomain. *Nat. Struct. Biol. 4*, 180–184.
9. Vardar, D., Buckley, D. A., Frank, B. S., and McKnight, C. J. (1999) NMR structure of an F-actin-binding "headpiece" motif from villin. *J. Mol. Biol. 294*, 1299–1310.
10. Bi, Y., Cho, J. H., Kim, E. Y., Shan, B., Schindelin, H., and Raleigh, D. P. (2007) Rational design, structural and thermodynamic characterization of a hyperstable variant of the villin headpiece helical subdomain. *Biochemistry 46*, 7497–7505.
11. Chiu, T. K., Kubelka, J., Herbst-Irmer, R., Eaton, W. A., Hofrichter, J., and Davies, D. R. (2005) High-resolution x-ray crystal structures of the villin headpiece subdomain, an ultrafast folding protein. *Proc. Natl. Acad. Sci. U.S.A. 102*, 7517–7522.
12. Wang, M., Tang, Y., Sato, S., Vugmeyster, L., McKnight, C. J., and Raleigh, D. P. (2003) Dynamic NMR line-shape analysis demonstrates that the villin headpiece subdomain folds on the microsecond time scale. *J. Am. Chem. Soc. 125*, 6032–6033.
13. Tang, Y. F., Goger, M. J., and Raleigh, D. P. (2006) NMR characterization of a peptide model provides evidence for significant structure in the unfolded state of the villin headpiece helical subdomain. *Biochemistry 45*, 6940–6946.
14. Xiao, S. F., Bi, Y., Shan, B., and Ralelgh, D. P. (2009) Analysis of core packing in a cooperatively folded miniature protein: the ultrafast folding villin headpiece helical subdomain. *Biochemistry 48*, 4607–4616.
15. Woll, M. G., Hadley, E. B., Mecozzi, S., and Gellman, S. H. (2006) Stabilizing and destabilizing effects of phenylalanine → F_5-phenylalanine mutations on the folding of a small protein. *J. Am. Chem. Soc. 128*, 15932–15933.
16. Zheng, H., Comeforo, K., and Gao, J. M. (2009) Expanding the fluorous arsenal: tetrafluorinated phenylalanines for protein design. *J. Am. Chem. Soc. 131*, 18–19.
17. Reiersen, H., and Rees, A. R. (2001) The hunchback and its neighbours: proline as an environmental modulator. *Trends Biochem. Sci. 26*, 679–684.
18. Hutchinson, E. G., and Thornton, J. M. (1994) A revised set of potentials for β-turn formation in proteins. *Protein Sci. 3*, 2207–2216.
19. Wilmot, C. M., and Thornton, J. M. (1988) Analysis and prediction of the different types of β-turn in proteins. *J. Mol. Biol. 203*, 221–232.
20. Richardson, J. S., and Richardson, D. C. (1988) Amino acid preferences for specific locations at the ends of α helices. *Science 240*, 1648–1652.
21. DeRider, M. L., Wilkens, S. J., Waddell, M. J., Bretscher, L. E., Weinhold, F., Raines, R. T., and Markley, J. L. (2002) Collagen stability: insights from NMR spectroscopic and hybrid density functional computational investigations of the effect of electronegative substituents on prolyl ring conformations. *J. Am. Chem. Soc. 124*, 2497–2505.
22. Shoulders, M. D., and Raines, R. T. (2009) Collagen structure and stability. *Annu. Rev. Biochem. 78*, 929–958.
23. Bretscher, L. E., Jenkins, C. L., Taylor, K. M., DeRider, M. L., and Raines, R. T. (2001) Conformational stability of collagen relies on a stereoelectronic effect. *J. Am. Chem. Soc. 123*, 777–778.
24. Shoulders, M. D., Satyshur, K. A., Forest, K. T., and Raines, R. T. (2010) Stereoelectronic and steric effects in side chains preorganize a protein main chain. *Proc. Natl. Acad. Sci. U.S.A. 107*, 559–564.
25. Chiang, Y. C., Lin, Y. J., and Horng, J. C. (2009) Stereoelectronic effects on the transition barrier of polyproline conformational interconversion. *Protein Sci. 18*, 1967–1977.
26. Horng, J. C., and Raines, R. T. (2006) Stereoelectronic effects on polyproline conformation. *Protein Sci. 15*, 74–83.
27. Kümin, M., Sonntag, L. S., and Wennemers, H. (2007) Azidoproline containing helices: stabilization of the polyproline II structure by a functionalizable group. *J. Am. Chem. Soc. 129*, 466–467.
28. Kim, W., McMillan, R. A., Snyder, J. P., and Conticello, V. P. (2005) A stereoelectronic effect on turn formation due to proline substitution in elastin-mimetic polypeptides. *J. Am. Chem. Soc. 127*, 18121–18132.
29. Naduthambi, D., and Zondlo, N. J. (2006) Stereoelectronic tuning of the structure and stability of the Trp cage miniprotein. *J. Am. Chem. Soc. 128*, 12430–12431.
30. Pace, C. N. (1986) Determination and analysis of urea and guanidine hydrochloride denaturation curves. *Methods Enzymol. 239*, 266–280.
31. Wüthrich, K. (1986) NMR of amino acid residues and mononucleotides, in NMR of Proteins and Nucleic Acids, pp 13−25, Wiley, New York.
32. Aune, K. C., Salahuddin, A., Zarlengo, M. H., and Tanford, C. (1967) Evidence for residual structure in acid- and heat-denatured proteins. *J. Biol. Chem. 242*, 4486–4489.
33. Deshpande, R. A., Khan, M. I., and Shankar, V. (2003) Equilibrium unfolding of RNase Rs from *Rhizopus stolonifer*: pH dependence of chemical and thermal denaturation. *Biochim. Biophys. Acta 1648*, 184–194.
34. Farruggia, B., and Picó, G. A. (1999) Thermodynamic features of the chemical and thermal denaturations of human serum albumin. *Int. J. Biol. Macromol. 26*, 317–323.
35. Tang, Y., Rigotti, D. J., Fairman, R., and Raleigh, D. P. (2004) Peptide models provide evidence for significant structure in the denatured state of a rapidly folding protein: the villin headpiece subdomain. *Biochemistry 43*, 3264–3272.
36. Janesko, B. G., Gallek, C. J., and Yaron, D. (2003) Using constrained schrödinger equations to separate resonant and inductive substituent effects: a new methodology for parametrizing simple models in chemistry. *J. Phys. Chem. A 107*, 1655–1663.
37. Alabugin, I. V., and Zeidan, T. A. (2002) Stereoelectronic effects and general trends in hyperconjugative acceptor ability of σ bonds. *J. Am. Chem. Soc. 124*, 3175–3185.
38. Kotch, F. W., Guzei, I. A., and Raines, R. T. (2008) Stabilization of the collagen triple helix by *O*-methylation of hydroxyproline residues. *J. Am. Chem. Soc. 130*, 2952–2953.